Testing Unified X-ray/UV Absorber Models with NGC5548

Smita Mathur, Martin Elvis and Belinda Wilkes
Harvard-Smithsonian Center for Astrophysics
60 Garden St, Cambridge MA 02138
Internet: smita@cfa.harvard.edu

June 1, 1995

Abstract

The bright Seyfert galaxy NGC5548 shows absorption features in its X-ray and UV spectra. The large amount of optical/UV and X-ray monitoring data available for this object makes it an ideal candidate to test our model of a common X-ray/UV absorber. We show that the UV/X-ray absorption is caused by a highly ionized (2.2< U <2.8) high column density ($N_H = 3.8 \times 10^{21}\ cm^{-2}$) gas situated outside the CIV emitting region ($2 \times 10^{16} < r_{abs} < 2 \times 10^{18}\ cm$). The gas is outflowing with a mean velocity of 1200±260 $km\ s^{-1}$ and corresponding kinetic luminosity of $\sim 10^{43} ergs^{-1}$. The gas is more highly ionized and has a much larger column density than earlier estimates based on UV data alone. This third example of an X-ray/UV absorber reinforces our earlier conclusion that outflowing, highly ionized gas is common in the inner regions of quasars.

1 Introduction

Recently we found that the ionized ("warm") X-ray absorbers and the associated UV absorbers were due to the same material in two radio-loud quasars: an X-ray quiet quasar 3C351 (Mathur *et al.* 1994) and a red quasar 3C212 (Mathur 1994). In both cases the absorber is situated outside the broad emission line region (BELR), is outflowing, and is highly ionized. While this result delineates a new nuclear component in lobe-dominated radio-loud quasars, it would clearly be much more interesting if the same component were present in all quasars and active galactic nuclei (AGN) with both X-ray and UV absorption (Ulrich 1988). In this paper we test this generalization by applying the same model to the best studied of all AGN, NGC 5548.

NGC 5548, a radio quiet Seyfert 1 galaxy, provides the best test case for the equivalence of the X-ray and UV absorbers and will yield a highly constrained determination of the physical properties of the absorber. This is because NGC 5548 has been extensively studied in reverberation mapping experiments in the optical and UV (Peterson *et al.* 1992, Clavel *et al.* 1991, Korista *et al.* 1995). These have led to the accurate determination of the physical size of the BELR. NGC 5548 has both an X-ray ionized absorber (Nandra *et al.* 1991, Fabian *et al.* 1994a) and an UV absorber (Shull & Sachs 1993), and the reverberation observations place limits on the response time of the UV absorbers to changes in the UV continuum. Note that this response time is due to the physical conditions of the absorber only since there is no light-travel-time delay along the line of sight.

We apply the photoionization modeling method of Mathur et al (1994) to the X-ray and UV absorbers in NGC 5548 to determine whether consistent values for abundances of all the observed ions can be obtained. In NGC 5548 the model must meet two extra requirements: it must not lead to a density for the absorber in conflict with its recombination time; and the distance of the absorber from the continuum source must not conflict with the well-determined BELR size.

2 Data

2.1 X-ray Data

X-ray observations of NGC 5548 have revealed a complex spectrum. EXOSAT showed that the source has a strong soft excess (Branduardi-Raymont 1986, 1989). *Ginga* showed, moreover that the X-ray spectrum and flux were variable (Nandra *et al.* 1991) and that the X-ray variability was correlated with the ultraviolet variability (Clavel *et al.* 1992). In addition, complex absorption was observed by *Ginga* with a possible Fe-K edge at ~8 keV, corresponding to an intermediate ionization stage of iron (~FeXX) with $\tau_{Fe-K} \sim 0.03$, and variable soft X-ray absorption. ROSAT observations of NGC 5548 (1990 July 16-21) showed an absorption feature in its X-ray spectrum arising from highly ionized oxygen, demonstrating the presence of an ionized absorber; E=0.81 ± 0.06 keV, $\tau = 0.35 \pm 0.13$ (Nandra *et al.* 1993)

Recent observations with ASCA (1993 July 28) confirmed the presence of an ionized absorber (Fabian *et al.* 1994a). OVII and OVIII absorption edges observed at 0.72 keV and 0.86 keV respectively were resolved in the ASCA spectrum. The optical depths of the edges were $\tau_{OVII} = 0.26^{+.04}_{-.08}$ and $\tau_{OVIII} = 0.12^{+.07}_{-.03}$. The combined OVII and OVIII opacity from ASCA agrees well with that observed with ROSAT. An equivalent hydrogen column density was $N_H = 3.8 \times 10^{21} cm^{-2}$. However the presence of an Fe-K edge is not confirmed ($\tau_{Fe-K} \leq 0.1$).

The absorption cross-sections of OVII and OVIII are $0.28 \times 10^{-18} cm^2$ and $0.098 \times 10^{-18} cm^2$ respectively (CLOUDY version 80.06, Ferland 1991). The column densities in the two ions are thus $N_{OVII} = 0.93^{+0.14}_{-0.29} \times 10^{18} cm^{-2}$ and $N_{OVIII} = 1.22^{+0.72}_{-0.30} \times 10^{18} cm^{-2}$. Given the total hydrogen column density and the solar abundance of oxygen relative to hydrogen ($= 8.51 \times 10^{-4}$, Grevesse & Andres 1989) the fraction of oxygen in the two stages of ionization is calculated; $f_{OVII} = 0.29^{+.04}_{-.09}$ and $f_{OVIII} = 0.38^{+.22}_{-.10}$. The absorber must thus be highly ionized to have 2/3 of the oxygen in hydrogen-like and helium-like states.

2.2 Ultraviolet Data: IUE

NGC 5548 has been studied extensively in the ultraviolet (Clavel *et al.* 1991, Korista *et al.* 1995). The UV spectrum shows absorption lines of CIV and

NV within the profiles of their broad emission lines (Shull and Sachs 1993; hereafter SS). The source was found to be highly variable in its continuum flux and also in the strengths of its emission and absorption lines. The UV continuum was found to vary by a factor of ~ 3 while the CIV absorption line EW varied by a factor of ~ 2 over a period of about 10 days. There is no observed lag between the variations in the continuum and the equivalent width (EW) of the CIV absorption line ($\Delta t \leq 4$ days, SS). Note that any delay between the continuum and absorption line variability is *not* due to light travel time (reverberation) effects, which are not operative along the line of sight. It is instead due to physical conditions within the absorber, specifically, the recombination time (see sec. 3.4). SS also infer a blueshift of 1200$\pm$260 km s^{-1} with respect to the systemic velocity of NGC 5548. We note that the earliest IUE spectra of NGC 5548 are also suggestive of an absorption feature at this position (Wu, Boggess and Gull 1981, Ulrich and Boisson 1983). We re-analyzed the 1979 IUE data (SWP05500, SWP05687, SWP05688, SWP05689, SWP07345, SWP073930) including those reported by Wu *et al.* (1981) using current extraction techniques . The CIV absorption line is present at similar velocity and of comparable strength to the later data (SS).

No associated Lyα absorption has been reported in the large literature on NGC 5548. Observationally it is difficult because the Lyα emission line of this low redshift source lies very close to geo-coronal Lyα. Theoretically, Lyα absorption was not expected (SS) as the absorbing gas was considered "fully ionized" in hydrogen. As a result all the published spectra cut off the blue wing of Lyα in the AGN emission line in order to remove geo-coronal Lyα from the spectrum, cutting out also part of the Lyα absorption line.

Because our models predict significant Lyα absorption, we retrieved and re-analyzed a set of IUE spectra taking care to go to shorter wavelengths. In Figure 1 we present an IUE spectrum of NGC 5548, without removing the geo-coronal Lyα. This clearly shows the presence of a Lyα absorption line at a redshift consistent with that of the other absorption lines.

2.3 Ultraviolet Data: HST

NGC 5548 was observed daily for a total of 39 times by HST in 1993 April/May to monitor the variability of the source in the ultraviolet (1140Å$< \lambda <$2312Å, Korista *et al.* 1995). HST FOS resolution is $\sim$1Å over this wavelength range (c.f. ∼6Å with IUE). Figures 2 a,b show the emission and absorption line profiles of Lyman-α and CIV respectively for the mean FOS spectrum. This spectrum was constructed by joining the combined G130H and G190H spectra; no scale factors were applied (see sec 2.4, Korista *et al.*1994). We measured the EWs of the absorption lines both in the individual HST spectra and in the mean. The CIV doublet $\lambda\lambda 1548, 1551$ is resolved with EW = 0.32±0.1Å and 0.08±0.03Å respectively in the mean FOS spectrum (Table 1). The measurement of absorption lines situated within a broad emission line profile is notoriously difficult, since the real shape of the emission line is unknown. We estimated the magnitude of our errors by making maximal, minimal and optimal measurements in each case (see e.g. figure 2a). This yielded a typical error of about a factor of two in individual spectra and about 30% error in the mean FOS spectrum. The N V doublet is also resolved in the HST data with EW = 0.1 and 0.04 (± 30%) in the mean spectrum.

An associated Lyα absorption line, at the same relative blueshift (Δz = 0.002) as the CIV-NV absorption system, is clearly seen with EW 0.5± 0.3 Å; a minimum HI column density is thus $N_{HI} \geq 4 \times 10^{13}$ cm^{-2}. There is another absorption feature immediately shortward ($\lambda_{\rm obs}$ = 1231.9, Δz = 0.004, EW $\sim$ 0.6). There are no corresponding CIV or NV absorption features at a similar relative blueshift and it appears to be unrelated to the associated absorption system we discuss here. The uncertainty in the Lyα EW is large due to its proximity both to this nearby absorption feature and to the peak of the emission line profile.

Note that the CIV EW in the mean HST spectrum is significantly lower than those reported for the IUE spectra (2 or 8Å SS) in 1989. The larger of the two SS EW values was derived by assuming that much of the emission line peak was absorbed. This is clearly not the case in the higher resolution HST data. The HST spectra also show that the absorption feature covers a smaller range in wavelength than was apparent from the IUE data. We re-measured nine IUE spectra around JD2447580, the time of the maximum continuum change, using $\Delta\lambda$ ∼10Å, rather than the 16Å used by SS. The exact wavelengths varied due to the inherent uncertainty in the wavelength calibration for spectra observed with the large IUE aperture. Our EW values are systematically smaller than SS's small values for the same spectra by a factor 0.6. We use our revised measurements for the remainder of this paper. We note that the 1989 IUE CIV EW are still larger that the HST values.

This may be due to the measurement difficulties in the low resolution IUE spectra.

3 Models

In the context of photoionization models we look for an ionized absorber that satisfies the X-ray constraints. Photoionization models predict the fraction of atoms in each ionization state, f_{ion}, given the column density (N_H), density (n) and ionization parameter ($U=\frac{Q}{4\pi r^2 n_H c}$, where Q is the number of ionizing photons) of a cloud of gas exposed to a continuum source with a defined continuum shape. All the photoionization calculations in this paper were performed using CLOUDY (Ferland 1991).

Mathur *et al.* (1994) have shown that the particular spectral energy distribution (SED) of each AGN should be used, rather than a 'typical' quasar SED as this might lead to incompatible physical conditions in a photoionized cloud. The observed radio to X-ray continuum of NGC 5548 is shown in figure 3 (data from Ward *et al.* 1987, SS 1993, Korista *et al.* 1995, Nandra *et al.* 1991). The continuum is corrected for Galactic reddening by E(B-V)=0.033 assuming a fixed conversion of $N_H/E(B-V) = 5.0 \times 10^{21}$ cm^{-2} mag^{-1} and N_H (1.65×10^{20} cm^{-2}, Nandra *et al.* 1993). The shape of the IR/optical continuum is similar to a typical AGN (Elvis *et al.* 1994) with the IR break shifted shortward to $100 \mu m$. The standard radio-quiet AGN continuum used by Mathews & Ferland (1987) is shown for comparison as a dashed line. NGC 5548 is much brighter in the X-rays than a typical AGN, but has a normal X-ray spectral slope, $\alpha_E = 0.8 \pm 0.2$ in the $2-10$ keV range (Nandra *et al.* 1991). In addition, it has a soft X-ray excess which can be approximated by a black body spectrum of temperature 150,000 K (dotted line in Figure 3). The heavy solid line in figure 2 shows the adopted input continuum. The X-ray column density N_H was fixed at the observed ASCA value of 3.8×10^{21} cm^{-2} (Fabian *et al.* 1994a).

3.1 The X-ray Absorber

Figure 4 shows the ionization fractions of OVII and OVIII as a function of U, using the de-reddened continuum for NGC 5548 and assuming solar abundances (Grevesse & Andres 1989). The number of ionizing photons, Q=$2.5h_{50}^{-2} \times 10^{54}$ s^{-1} where h_{50} is the Hubble constant in the units of 50 km s^{-1} Mpc^{-1}. Note that this value of Q is in fact smaller than that used by Ferland *et al.* 1992, Q=$4h^{-2} \times 10^{54}$ s^{-1}, which is based on a scaled version of the standard continuum. This is because most of the ionizing photons come from the energy range 1–20 Rydberg where the standard continuum is brighter (figure 3). The observed values are highlighted with thick lines. Using the constraints on the fractional ionization of OVII and OVIII from the ASCA data ($\tau_{OVII} = 0.29^{+0.04}_{-0.09}$, $\tau_{OVIII} = 0.38^{+0.22}_{-0.09}$, Fabian et al 1994a, section 2.1) the allowed range of the ionization parameter is narrow, $2.2 < U < 2.8$. (Note that this is a *linear* scale.) If instead the observed continuum is used, i.e. with no reddening correction, the inferred range changes to $1.2 < U < 1.3$ and the dependence of $log f_{ion}$ on U remains qualitatively the same. In the rest of the paper we quote all the parameters only for the reddening corrected SED. The values of ionization fraction are independent of the gas density and so, the density (n) is not constrained by photoionization models alone (see sec. 3.4). Density n = 10^7 atoms cm^{-3} was used in the input to CLOUDY.

We investigated whether the lack of an Fe/K absorption feature observed by ASCA (section 2.1) is consistent with our model. The $\sim$ 8 keV Fe-K absorption edge would most likely be due to an intermediate ionization stage of iron $\sim FeXX$ (Nandra *et al.* 1991), most likely FeXVII, since it dominates over a wider range of U than other ionization state, since it is neon-like and so more stable than other iron ions.

We find that, for the best fit model for the oxygen edges, the dominant stage of iron is indeed FeXVII, log $f_{FeXVII} = -0.77$, implying N$_{FeXVII}$ < $2.2 \times 10^{18} cm^{-2}$. The ASCA upper limit to an Fe-K edge is $\tau < 0.1$ (section 2.1), so N$_{FeXVII} = 3 \times 10^{16}$ cm^{-2}, assuming solar abundance of iron (4.68×10^{-5}, Grevesse & Andres 1989). This is consistent with the absence of any Fe-K X-ray absorption edges. This absorption system, however, falls short by a factor of $\sim$ 25 of producing the large observed EW of the Fe-K emission line even for a uniform spherical shell (model EW $\sim$7 eV, observed EW = 180 $\pm$60 eV); consistent with the conclusion of Nandra *et al.* (1991).

3.2 Combined X-ray and UV constraints

We follow the technique developed in Mathur *et al.* (1994) to look for an absorption system that satisfies both X-ray and UV constraints. The X-ray constraints require 2.2<U<2.8, as discussed above. Thus, if the X-ray and UV absorbers are one and the same (as was found to be the case in 3C351 and 3C212) in NGC 5548, then it can be seen from figure 3 that the ionization fraction of CIV is constrained to be $f_{CIV} = 2.0^{+0.5}_{-0.4} \times 10^{-4}$ ($\log f_{CIV} = -3.7^{+0.2}_{-0.3}$).

In the mean HST spectrum, the CIV doublet ratio is 3.8±0.2, thus the CIV absorption lines lie off the linear portion of the curve of growth (see e.g. Spitzer 1978, Weise *et al.* 1966). In figure 5a,b,c the curves of growth for velocity spread parameters b=20, 40, 60, 80 km s^{-1} are shown. Figure 4a shows the observed equivalent width for CIV (Table 2) and the constraint on log(n$f\lambda$) derived from the X-ray constraint on f_{CIV} (see above) assuming a solar abundance for carbon (3.63×10^{-4}, Grevesse & Andres 1989) and oscillator strength f=0.285 (Allen 1973). Similar plots (Figures 5b, c) for NV (at solar abundance, 3.63×10^{-4}, Grevesse & Andres 1989) and Lyman-α (using oscillator strengths of 0.235 and 0.4162 for NV and Lyman-α respectively, Allen 1973) lead to the allowed b values given in Table 2. A consistent solution for all three ions is obtained for b=40km s^{-1}, with a small tolerance for both UV and X-ray constraints to be met.

The measured line widths for the CIV doublet are $\sim$ 350 km s^{-1} (FWHM), broader that the nominal spectral resolution for this observation and thus possibly resolved. This would imply that the absorber is dispersed in velocity space (see also SS). However we note that the resolution of the FOS using the 4.3" slit (as in this case) is not well-defined. In particular $\sim$ 50% of the light is in very broad wings (Korista, private communication) and thus we cannot be certain that the line is resolved from these data. As discussed in section 2.3, the uncertainty in the Lyα EW is large, leading to a large uncertainty in the HI column density: $13 < logN_{HI} < 18$ while the model value ranges from 15.2 to 15.4 (Table 2). An actual HI column density in the higher end of the observed range would imply that the heavy element abundance in the X-ray/UV absorber is depleted. Conversely, if it is in the lower end of the range enhanced metal abundance is implied. A Lyman edge absorption would be observed if N_{HI} is large ($logN_{HI} > 16.3$). The recent HUT observations (Spring 1995) will be able to detect such a Lyman edge.

The ASCA observations were made on 1993 July 28, while the HST observations were made between 1993 April and 1993 May. The close agreement of U from the ASCA and HST data requires that the UV continuum flux is similar in both observations. The optical light curve of NGC 5548 (Korista *et al.* 1995) shows that the mean continuum level during the HST observations ($f_\lambda(5100\AA) = 9.14 \times 10^{-15}$erg s^{-1} cm^{-2} Å^{-1}) was indeed only 4% below the continuum at the time of the ASCA observations ($\sim 9.4 \times 10^{-15}$ erg s^{-1} cm^{-2} Å^{-1}).

One additional consistency check is possible. In a highly ionized system such as this, magnesium is highly ionized (MgVI and higher) leaving no magnesium in the MgII state ($\log f_{MgII} < -30$) and thus MgII absorption should not occur. This is consistent with the observations (sec. 2.2).

Thus we have a single consistent model that simultaneously, correctly predicts the fractional ionization of OVII, OVIII, NV, CIV, HI and FeXVII and the lack of presence of MgII and other low ionization species. We conclude that the UV and X-ray absorbers in NGC 5548 are one and the same.

3.3 Variability

Our photoionization model of the UV absorber in NGC 5548 must explain the observed variability of the CIV absorption line (SS) assuming that their relative measurements are correct (see section 2.3). As can be seen from figure 5, the absorption line lies slightly off the linear part of the curve of growth. The slope of the curve of growth in that region is about 0.5. Since this is a log-log plot a factor of two change in the column density of the CIV ion would result in a factor of 1.4 change in the EW of the line. In our model, the variations in N_{ion} are caused by variations in the ionization parameter of the absorber (figure 4) which is directly proportional to the variations in the ionizing flux. An increase in U results in a decrease in N_{CIV} (figure 3). Our measurements of the IUE data show the continuum at 1500Å varying from 2.0×10^{-14} to 4.7×10^{-14}erg cm^{-2} s^{-1}Å^{-1}, a factor 2.4, while the CIV absorption line EW changes from 1.9±0.3 to 1.4±0.4Å, consistent with the model prediction of a factor 1.5.

During the HST observations the maximum continuum variations were only a factor of ~ 1.5 (Figure 6). There is no obvious variability observed in the CIV absorption line EW. Unfortunately the errors in the CIV EW are large, due to the inherent measurement difficulty discussed earlier (sec. 2.3) The two solid lines indicate the variability predicted by our model based on the observed continuum variations and both zero time lag and a time lag of two days. The data are certainly consistent with the model ($\chi^2 = 6.05$ for 35 degrees of freedom); however no strong conclusions can be drawn.

3.4 Physical Properties of the Absorber

The X-ray/UV absorber in NGC 5548 shows absorption features due to Lyα, NV, CIV, OVII, OVIII and Fe-XVII. The X-ray and UV constraints can now be combined to derive the physical properties of the absorber. It is highly ionized ($2.2 < U < 2.8$) and has a large column density ($N_H = 3.8 \times 10^{21} cm^{-2}$). The CIV recombination time must be shorter than the variability response timescale of $\leq$4 days (SS), which sets a lower limit to the density of the absorber; n$\gtrsim 5 \times 10^5 t_4^{-1} cm^{-3}$, where t_4 is the lag between the continuum and absorption line variation in units of 4 days. The thickness of the absorbing slab is then $\Delta r \lesssim 8 \times 10^{15} cm$. It is outflowing with a mean velocity of $v_{\rm out} = 1200 \pm 260 kms^{-1}$ as inferred by its blueshift with respect to the systemic velocity of the galaxy (SS) and possibly dispersed in velocity (FWHM $\sim 300 km\ s^{-1}$).

The radial distance of the absorber $r_{abs} = (Q/4\pi U n_H c)^{1/2}$ is $\lesssim$0.7 – 0.8 $t_4^{1/2}$ pc given the above density constraint. The maximum depth of the CIV absorption line during the IUE observations is greater than the continuum level (SS). This implies that the absorber at least partially covers the CIV emitting region whose size has been accurately determined for NGC 5548 = 7.5$\pm$0.5 lt. days. Combining these two limits gives $8\ lt.\ days < r_{abs} < 0.8\ pc.$, i.e. $2 \times 10^{16} < r_{abs} < 2 \times 10^{18} cm$.

The lower limit on r_{abs} limits the density to n$< 5 \times 10^9\ cm^{-3}$. The density is thus constrained to be $5 \times 10^5 t_4^{-1} < n < 5 \times 10^9\ cm^{-3}$. The radial distance and density are not strongly constrained, nor are the model constraints in conflict with those from the variability data.

Associated absorption has been observed in $\sim$ 10% of Seyfert 1 galaxies (Ulrich 1988) which implies $\sim$ 10% covering factor of the absorber in all Seyfert 1s. If we assume this covering factor, $f_{0.1}$, applies to NGC 5548 then the mass of the absorber is $\rm M_{abs} \sim 20 f_{0.1} M_{\odot}$. The mass outflow rate can be calculated, by assuming uniform density: $\dot{\rm M}_{out}$=$\rm M_{abs} v_{out} \Delta r^{-1} f_{0.1}$ =10 $f_{0.1} M_{\odot} yr^{-1}$. This is an upper limit in that the absorber is much thinner than its radius from the center, so that the time averaged $\dot{\rm M}_{out}$ is likely to be much smaller. The same rate is a lower limit in that we measure only the velocity component in our line of sight (see sec. 4.4). This mass outflow rate is quite a bit larger than the accretion rate of 0.08 $M_{\odot} yr^{-1}$ needed to power the $\rm L_{Bol} = 5 \times 10^{44}$ erg s^{-1} continuum source at 10% efficiency. The outflow would carry a kinetic luminosity of $\dot{\rm M}^2_{out} v^2_{\rm out}/2 = \sim 10^{43}$ erg s^{-1} about fifty times lower than the radiative luminosity of NGC 5548. A summary of the properties of the absorber is given in Table 3.

4 Discussion

4.1 Comparison with Previous models

The combination of X-ray and improved UV constraints from HST have led to derived conditions very different from those reported earlier by SS based on the IUE data alone. SS necessarily assumed CIV to be the dominant state of ionization (f_{CIV}= 0.1) leading to U $\sim 10^{-3}$. Combining this with the lack of MgII absorption led to N$_H < 10^{20.5}$ cm^{-2}. However in our model these parameters are constrained: 2.2< U <2.6, $-3.4 < f_{CIV} < -3.9$. We are thus led to conclude that the absorber is highly ionized and has a large column density (N$_H = 3.8 \times 10^{21}$ cm^{-2}, Fabian et al 1994a).

4.2 Generalizing UV/X-ray Absorbing Outflows

The physical properties of the long known UV absorber in NGC 5548 are now well constrained with the identification of a UV/ X-ray absorber. We can therefore generalize our unification of UV and X-ray absorbing outflows for lobe-dominated radio-loud quasars to include radio-quiet Seyfert galaxies, and most likely to all associated absorbers in AGN.

A strong correlation has been observed between the radio properties and associated absorption line properties of AGN: all Broad Absorption Line Quasars (BALQSOs) are radio-quiet (Stocke *et al.* 1992) and all MgII associated absorption line quasars are lobe-dominated and radio-loud (Aldcroft *et al.* 1994). Associated CIV absorbers are a mixture of lobe- and core-dominated radio-loud quasars, and radio quiet quasars. It is of interest to note that even though NGC 5548 is radio quiet, it is unusual in that its radio luminosity is dominated by the extended radio flux, which has a larger physical size than in any other radio quiet Seyfert galaxy (Wilson & Ulvestad 1982). In this respect it is similar to a lobe-dominated quasar, providing a link between lobe-dominated, radio loud AGN with associated absorption and radio-quiet AGN, perhaps also the BALQSOs. It further suggests that AGN with UV/X-ray absorbers are edge-on. To have an inclination indicator in radio-quiet AGN would be most valuable, and this possibility should be studied further.

4.3 Comments on variability in NGC 3227 and MCG-6-30-15

Variable X-ray spectra and the existence of ionized absorbers have been observed in two more AGN with ASCA: NGC 3227 (Ptak *et al.* 1994) and MCG-6-30-15 (Fabian *et al.* 1994b). In both cases the variations in the properties of the ionized absorbers were deduced to be incompatible with the variations seen in the continuum.

In NGC 3227 (Ptak *et al.* 1994) rapid flux variations were observed with a time scale of $\sim 10^4$ seconds. An OVI absorption edge was detected with opacity $\tau \sim 0.75$. The model fits to the spectra in high and low flux states showed that (1) for the same value of photon index Γ in both high and low states, N_H and U *decrease* when the luminosity increases; (2) for different Γs, the same N_H and U can be fitted in both high and low states. Both of these models seem unphysical and hence the authors suggested that a warm absorber model may be too simple.

This, however, may not be the case, since it does not allow for delays due to the recombination time of the absorber. The best fit τ in NGC 3227 is remarkably similar in both high and low states implying that the ionization structure of the absorber has not changed even though the luminosity has changed. This implies a recombination time of OVI $> 10^4$ seconds. For OVI, the recombination time, $T = 4.3 \times 10^4 n_6^{-1}$ sec. (Shull & Van Steenberg, 1982) where n_6 is the density in the units of 10^6 cm^{-3}. This implies a density of the warm absorber, n$< 10^6$ cm^{-3}. With the model value of U ~ 0.05 this places the absorber at r$= 10^{19}$cm, well outside the BELR (which would have a radius of 7×10^{15}cm, assuming an $L^{1/2}$ scaling from NGC 5548).

It should be noted that the physical parameter which responds to continuum variations is τ rather than U. Indeed, if τ remains the same while the luminosity increases, the fitted value of U, which assumes the system is in equilibrium, would necessarily decrease.

A similar apparent discrepancy was observed in MCG-6-30-15 (Fabian *et al.* 1994b) which has an OVII absorption edge. In this case τ decreased significantly over 23 days. The luminosity also decreased over this period, while the fitted value of the ionization parameter increased. Whether the change in τ correlates or anti-correlates with the change in luminosity depends upon U (see figure 3). The recombination time of OVII is $\sim 0.28 n_6^{-1}$ days (Shull & Van Steenberg, 1982). The data imply that t$\leq$ 23 days and so $n \geq 10^4 cm^{-3}$, a very reasonable constraint.

We argue that the warm absorber models in NGC 3227 and MCG-6-30-15 are *not* unphysical and that the data do not require more complex models. The information provided by the variability not only helps us understand this fact, but also provides an important constraint on the density of the absorber.

The low value of U for NGC 3227 (cf. 2.6 for NGC5548) implies a wide range of ionization states from object to object for the associated absorbers in radio-quiet AGN, as in radio-loud.

4.4 Implications for the Nature of the Outflowing Material

Now that we understand the physical properties of the absorber, we can begin to ask astrophysical questions.

The lack of differential time delays between the red and blue wings of the broad line profiles shows that the BELR motions are not primarily radial (Korista *et al.* 1995). Yet the absorbing material outside the BELR shows large outflows, both in NGC5548 and in the other UV absorbers (Ulrich 1988). How is the orbital or random motion at BELR radii converted to an organized flow? What is the driving force? The continuum radiation pressure acting on the partially ionized gas (Mathur *et al.* 1994, Turner *et al.* 1994) may play an important role. In a more specific scenario, Glenn, Schmidt & Foltz (1994) and Aldcroft et al (1995), have independently suggested that in BALQSOs and radio-loud quasars respectively we are looking almost edge-on at material blown off a dusty disk (which itself may be the BELR) by radiation pressure. Since there is some evidence that NGC5548 too is edge-on the same picture may apply there.

Material escaping vertically from an edge-on disk would then follow a path that is not purely radial as it is accelerated by the continuum radiation pressure. If the material originates at only a restricted range of radii in the disk, this could explain a number of otherwise puzzling features. In particular, the limited thickness of the absorber in NGC5548 cannot be understood in any continuous radial wind model. The X-ray column density directly rules out significant additional accelerated or decelerated material, unless it is fully stripped through iron (Nandra et al 1991). Only by making the wind intermittent, or by allowing for a velocity component in the plane of the sky (so moving the rest of the flow out of our line of sight) can we keep the thickness small.

Another consistency check is to confirm that the persistence of the absorber is consistent with the large observed outflow velocity (1200 ± 200 km s^{-1}). In the three years separating the ROSAT and ASCA observations no significant change in the OVII/OVIII opacity was detected. (ROSAT $\tau = 0.35 \pm 0.13$ (Nandra *et al.* 1993); ASCA $\tau = 0.38^{+0.08}_{-0.09}$ (Fabian *et al.* 1994a)). A formal 3σ upper limit for a change in τ is 0.27 (i.e. $\sim$80%). The distance traveled by the absorber in 3 years is 1.2×10^{16}cm. In order to limit a change in U to <80%, this must represent a <34% change in distance from the ionizing continuum (assuming a constant density system.) This leads to $r_{abs} \geq 3.5 \times 10^{16}$cm, slightly larger than the minimum distance determined from the size of the BELR (2×10^{16} cm, section 3.4), and so consistent with our earlier derived parameters for the absorber.

The first IUE observations, some 15 years ago, also showed a CIV absorber at a similar velocity and depth (section 2.2). These observations provide more constraints. The outflow cannot be intermittent if it has persisted for 15 years. Assuming a constant mean velocity for the absorber leads to a present minimum distance $r_{abs} > 5\times10^{16}$ cm, and a corresponding maximum density n$< 8\times10^{8}$ cm^{-3}. These are both consistent with the derived absorber parameters (section 3.4). However, if the apparent width of the absorption line in the HST data is real ($\sim$ 300 km s^{-1}) and represents the internal velocity dispersion of the gas over the past 15 years, then it will have led to a thickening by $\sim 10^{16}$ cm over 15 years, comparable with our estimate of the present absorber thickness ($< 8 \times 10^{15}$ cm, section 3.4). In which case the absorber would have had zero depth when IUE first observed it, which is unlikely since otherwise it has not changed significantly. This difficulty disappears if we are looking through a flow with a component in the plane of the sky, since then we are seeing a steady state flow crossing our path. This physical picture, derived from observations, is very similar to the wind models of BALQSOs by Murray *et al.* (1995).

Testing the model further in NGC5548 could be achieved by measuring the recombination time, and hence the absorber density. This implies a small sampling interval (< 1 day) accompanied by continuum changes by at least a factor of two. Monitoring the ionization parameter at a given continuum flux over a number of years to search for density changes would also test the model. High spectral resolution observations (e.g. with the HST GHRS) could examine the velocity structure of the absorber, and perhaps measure b values of any components. Tests for the edge-on nature of AGN with UV/X-ray absorbers also need to be pursued.

5 Conclusions

In this paper we have shown that the X-ray and UV absorption in NGC5548 can be explained quantitatively by having the same material produce the absorption features due to OVII, OVIII (in X-rays), CIV, NV, HI (in the UV), and not produce observable features due to FeXVII and MgII and other low ionization lines. This simple model passes further tests by not violating the size and density limits imposed by the reverberation mapping data. We conclude that the X-ray and UV absorption does indeed arise from the same material.

Combining the improved X-ray and UV constraints from ASCA and HST, together with the reverberation mapping variability constraints leads us to understand the physical properties of the absorber. The absorber is highly ionized ($2.2 < U < 2.8$), has high column density ($N_H = 3.8 \times 10^{21}\ cm^{-2}$), low density ($5 \times 10^5 t_4^{-1} < n < 5 \times 10^9\ cm^{-3}$), and is situated outside the CIV emitting region ($2 \times 10^{16} < r_{abs} < 2 \times 10^{18}\ cm$). The gas is outflowing with a mean velocity of $1200 \pm 200\ km\ s^{-1}$ and has a corresponding kinetic luminosity of $\sim 10^{43} ergs^{-1}$.

We can now generalize our unification of UV and X-ray absorbing outflows from the lobe dominated radio-loud quasars to include radio quiet Seyfert galaxies. This may also provide a link to the radio quiet BALQSOs. This analogy suggests that the UV/X-ray absorbers in radio-quiet AGN may be viewed close to edge-on, which would be a valuable known parameter if it can be independently supported. Now that we understand the physical properties of the absorber, we can begin to ask astrophysical questions, the dynamics of the outflow and its role in the circumnuclear region of AGNs. A scenario in which the absorbing material comes off a disk, and is accelerated by the radiation pressure of the continuum source may explain the persistence of the absorber in spite of its large velocity and thin shell-like geometry.

We thank Brad Peterson and Kirk Korista for valuable discussions and for early access to the HST spectra. We also thank Jonathan McDowell for his *Tiger* software. This work was supported in part by NASA Grant NAGW5-2201 (LTSA).

Table 1: Absorption Line Parameters

Line		λ_{obs}Å	EWÅ HST[a]	EWÅ IUE
CIV	1548.2	1572.4	0.30 ±0.10	1.6±0.3[b]
	1550.8	1575.4	0.08±0.03	
NV	1238.8	1260.7	0.04±0.01	–
	1242.8	1262.5	0.10 ±0.03	
Lyα		1234.1	0.5±0.3	–

a. in mean spectrum.
b. SS mean value scaled by our correction factor, 0.6 (see text).

Table 2: UV and X-ray constraints on b [a]

Ion	$\log(W_\lambda/lambda)$ (from UV)	$\log(N\lambda f)$ (from X-ray)	b (km s^{-1})
CIV	-3.61 ± 0.02	8.9−9.4	40−50
NV	-3.92 ± 0.03	8.5−9.1	18−40
HI	$-3.8^{+0.3}_{-0.2}$	9.9−10.1	20−60

a. Ranges are $\pm1\sigma$.

Table 3: Physical conditions of X-ray/UV absorber

Parameter	Constraint	Derived from:
Neutral hydrogen column density, N_H	$N_H \sim 3.8 \times 10^{21}$ cm^{-2}	X-ray (Fabian *et al.* 1994)
Ionization Parameter, U	$2.2 < U < 2.8$	τ(OVII,OVIII) X-ray (Fabian *et al.* 1994, Nandra *et al.* 1993)
Radial Distance, r_{abs}	2×10^{16} cm $< r_{abs} < 2 \times 10^{18}$ cm	LL: BELR covered (Peterson *et al.* 1993) UL: n, U
Density, n	5×10^5 cm^{-3} $\lesssim n < 5 \times 10^9$ cm^{-2}	LL: recombination time < 4 days (SS) UL: r_{abs}, U
Outflow velocity, v	1200 ± 260 km s^{-1}	Line redshift (SS)
Thickness, Δr	$\lesssim 8 \times 10^{15}$ cm	N_H, n
Mass	$\sim 20 f_{0.1}$ $M_\odot$	n, r_{abs}, Δr (covering factor, $f_{0.1} = 0.1$)

References:

Aldcroft, T & Elvis, M. & Bechtold, J. 1995 MNRAS submitted.
Allen, C. W. 1973, *Astrophysical Quantities* [The Athlone Press]
Arav, H. & Li, Z. 1994, Ap.J. 427, 700
Branduardi-Raymont, G. 1986 in *The Physics of Accretion onto Compact Objects*, eds: K. O. Mason, M. G. Watson & N. E. White., p. 407 [Springer-Verlag; Berlin]
Branduardi-Raymont, G. 1989 in *Active Galactic Nuclei* eds: D. E. Osterbrock & J. S. Miller, p. 177 [Kluwer]
Elvis, M., Wilkes, B. J., McDowell, J. C., Green, R. F., Bechtold, J., Willner, S. P., Cutri, R., Oey, M, S., & Polomski, E. 1994 ApJS, 95, 1
Clavel, J. *et al.* 1991 ApJ 366, 64
Clavel, J. *et al.* 1992 ApJ 393 , 113
Fabian, A., Nandra, K., Brandt, W., Hayashida, K., Makino, F. & Yamauchi, M., 1994a in *New Horizons in X-ray Astronomy*, eds. F. Makino and T. Ohashi, [Universal Academy Press: Tokyo], p573
Fabian, A. *et al.* 1994b, PASJ, 46, L59
Ferland, G. F. 1991 "HAZY", OSU Astronomy Department Internal Report
Grevesse, N., & Andres, E. 1989 in *Cosmic Abundances of Matter*, AIP Conference Proceedings, 183, 1. Ed. C. J. Waddington (New York: AIP)
Korista, K. *et al.* 1995, ApJS, in press (April 15)
Mathews, W. G. & Ferland, G. J. ApJ 323, 456
Mathur, S., Wilkes, B., Elvis M. & Fiore, F. 1994, ApJ, 434, 493
Mathur, S. 1994, ApJL, 431, L75
Murray, N., Chiang, J., Grossman, S. A., & Voit, G. M., 1995, ApJ, in press
Nandra, K. *et al.* 1991, MNRAS 248, 760
Nandra, K. *et al.* 1993, MNRAS 260, 504
Peterson, B. M. *et al.* 1992, ApJ 392, 470
Ptak, A., Yaqoob, T., Serlemitsos, P. J., Mushotzky, R., & Otani, C. 1994, Ap.JL, 436,
Shull, M. J. & Sachs, E. R. 1993, ApJ 416, 536
Shull, M. J. & Van Steenberg, 1982, ApJS, 48, 95
Spitzer, L. 1978 *Physical Processes in the Interstellar Medium*, [Wiley-Interscience], pp 46 – 57
Stocke, J. T., Morris, S. L., Weymann, R. J. & Foltz, C. B. 1992 Ap. J. 396, 487

Turner, T. J., Nandra, K., George, I. M., Fabian, A., & Pounds, K. A. 1994, ApJ 419, 127
Ulrich, M. H., 1988, MNRAS, 230, 121
Ulrich, M. H. & Boisson, C. 1983, ApJ, 267, 515
Ward, M., Elvis, M., Fabbiano, G., Carleton, N. P., Willner, S. P. & Lawrence, A. 1987, Ap. J. 315, 74
Wiese, W. L., Smith, M. W., & Glennon, B. M. 1966 *Atomic Transition Probabilities* [U.S. Government Printing Office]
Wilson, A. & Ulvestad, J. 1982, ApJ, 263, 576
Wu, C., Boggess, A., & Gull, T. 1981, ApJ, 247, 449

Figure Captions:

Figure 1: An IUE spectrum of NGC 5548 (an average of SWP35029, SWP35284, SWP35461, SWP35636, SWP35849, SWP36018, SWP36369, SWP36567 & SWP36715) showing the presence of Lyα absorption line.

Figure 2: An HST mean FOS spectrum of NGC 5548 showing (a) Lyα, NV and (b) CIV absorption troughs. In (a) we also indicate our maximal and minimal estimates of the absorption line strength (dashed line). The dotted line indicates the extrapolation to the observed line profile.

Figure 3: Spectral Energy Distribution of NGC 5548: the data are from Ward *et al.* (1987), SS (1993) and Nandra *et al.* (1991). The solid line represents our adopted SED. The dotted line is 150,000 K black body spectrum. The dashed line is a 'standard' AGN continuum shown for comparison (see text).

Figure 4: Ionization fractions of OVII, OVIII, CIV, NV and HI as a function of U. The thick lines mark the observed ranges for OVII and OVIII (ASCA). $\blacktriangle$: HST values for CIV and NV; $\circ$: IUE range. The HST range for HI is large (see text) represented by the thick curve. The vertical lines define the best fit model parameter: $2.2 < U < 2.8$.

Figure 5: The curve of growth for b values from 20 to 80 km s^{-1} in steps of 20 km s^{-1}. Horizontal lines are for the observed values of absorption lines in the mean HST spectrum; (a) CIV (b) NV and (c) Lyα.

Figure 6: Variability in the continuum and CIV absorption line EW during HST observations. Continuum is in arbitrary units. The dashed horizontal line is the mean EW. Two solid lines represent the predicted variability for no time lag and for a time lag of two days.

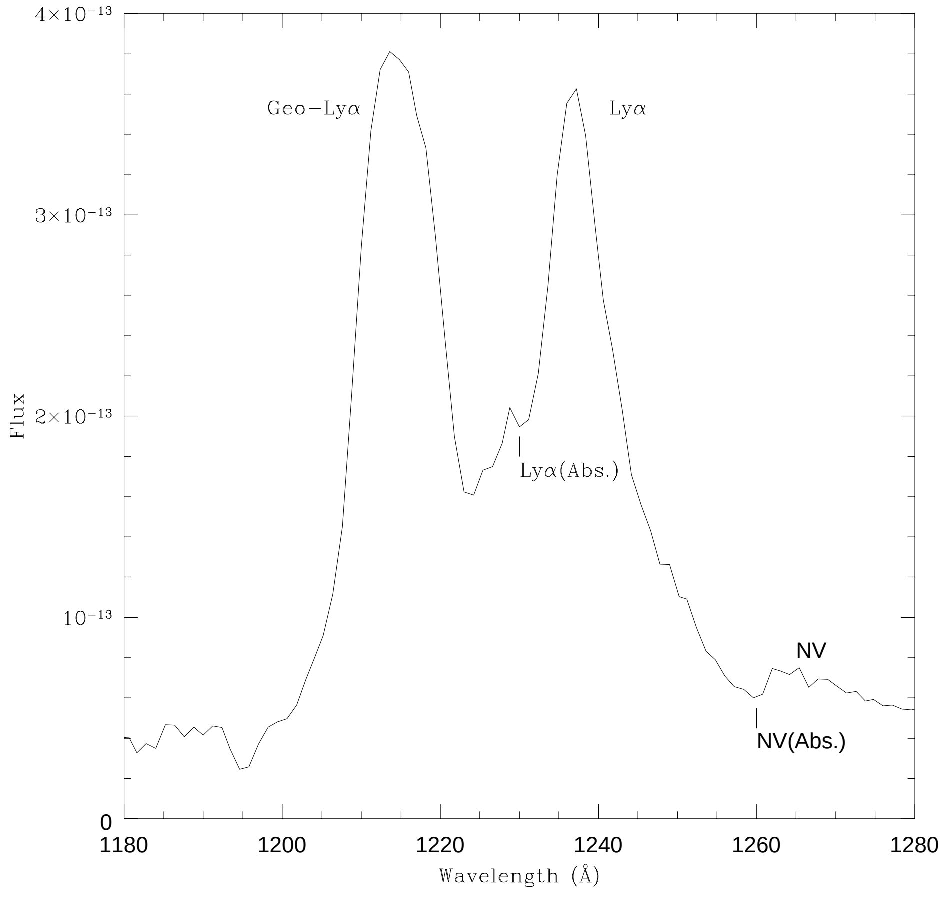

4×10⁻¹³
3×10⁻¹³
2×10⁻¹³
10⁻¹³
0
Flux
Geo−Lyα
Lyα
Lyα(Abs.)
NV
NV(Abs.)
1180
1200
1220
1240
1260
1280
Wavelength (Å)

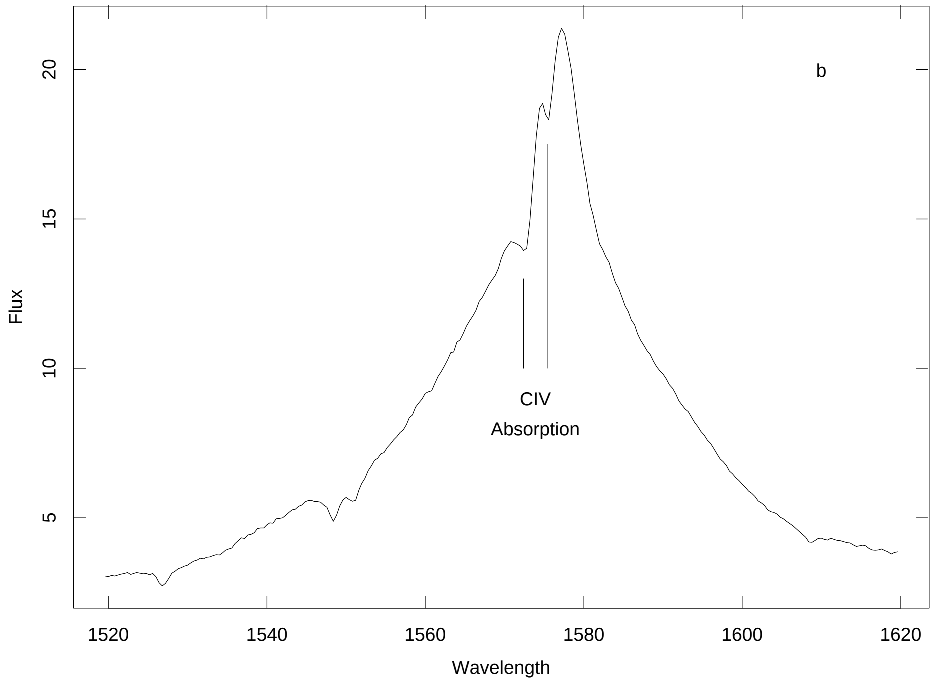
b
CIV
Absorption
Flux
Wavelength
5
10
15
20
1520
1540
1560
1580
1600
1620

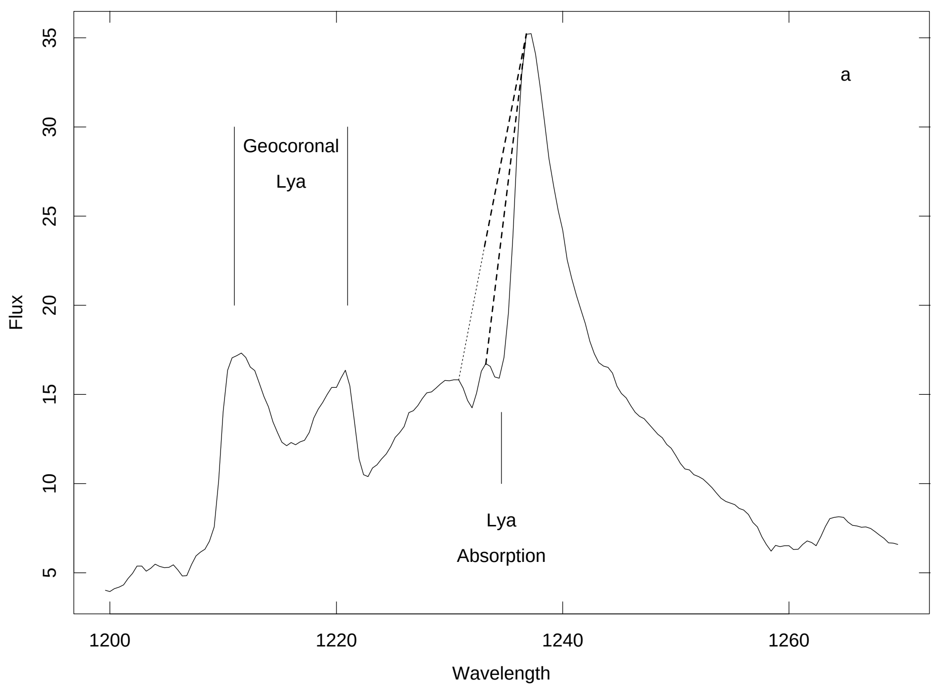

a
Geocoronal
Lya
Lya
Absorption
Flux
Wavelength
5
10
15
20
25
30
35
1200
1220
1240
1260

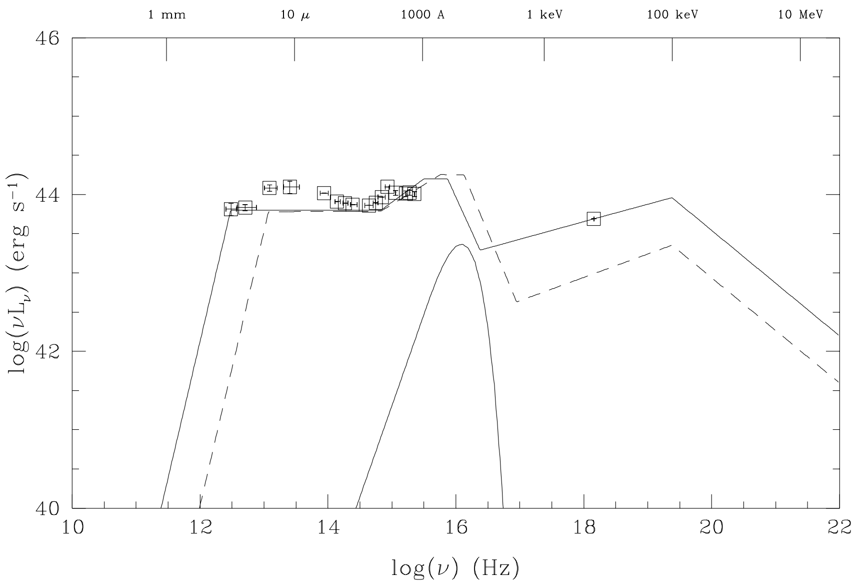

1 mm
10 μ
1000 A
1 keV
100 keV
10 MeV
46
44
42
40
10
12
14
16
18
20
22
log(νL_ν) (erg s^-1)
log(ν) (Hz)

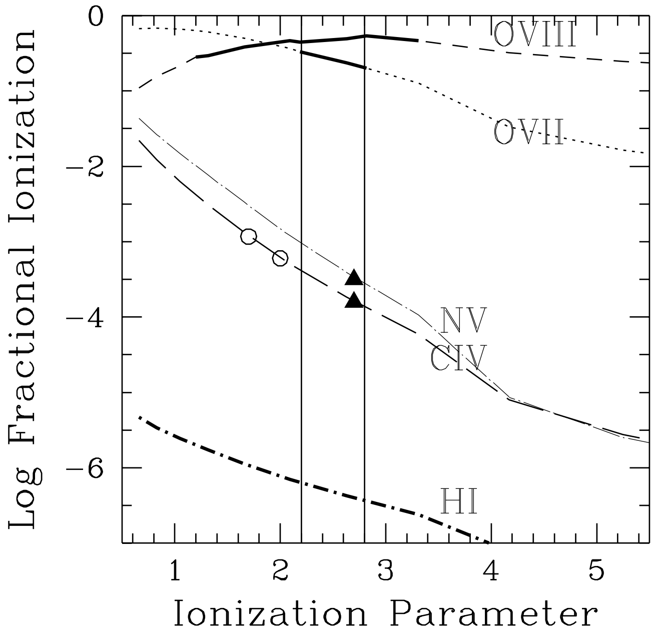

OVIII
OVII
NV
CIV
HI
0
−2
−4
−6
1
2
3
4
5
Log Fractional Ionization
Ionization Parameter

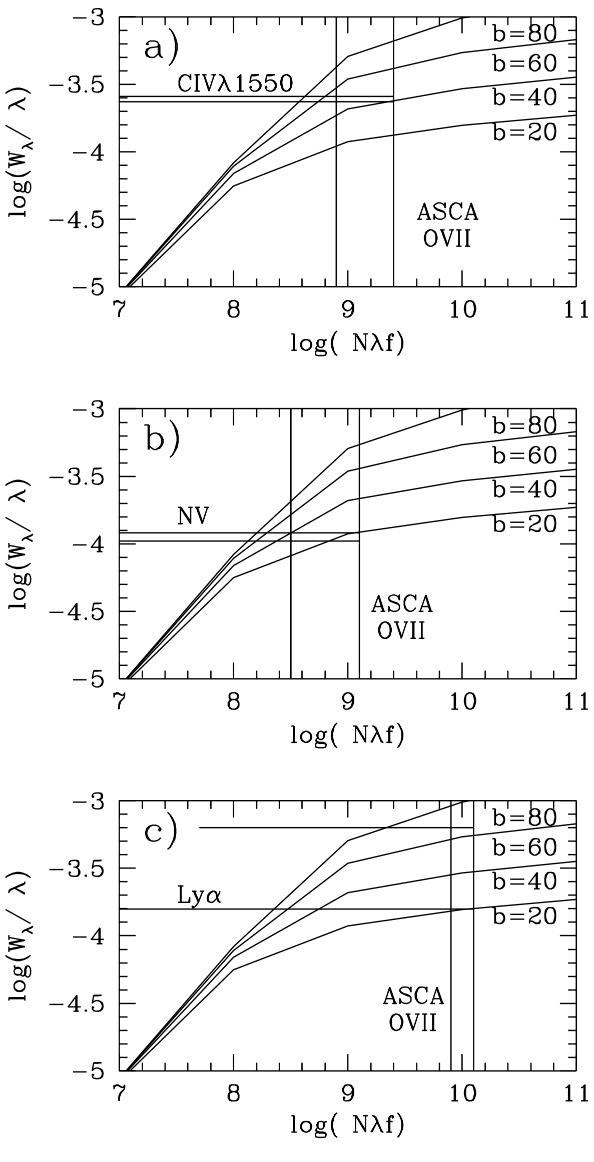
a)
b)
c)
CIVλ1550
NV
Lyα
b=80
b=60
b=40
b=20
ASCA
OVII
log(W_λ/ λ)
log(Nλf)

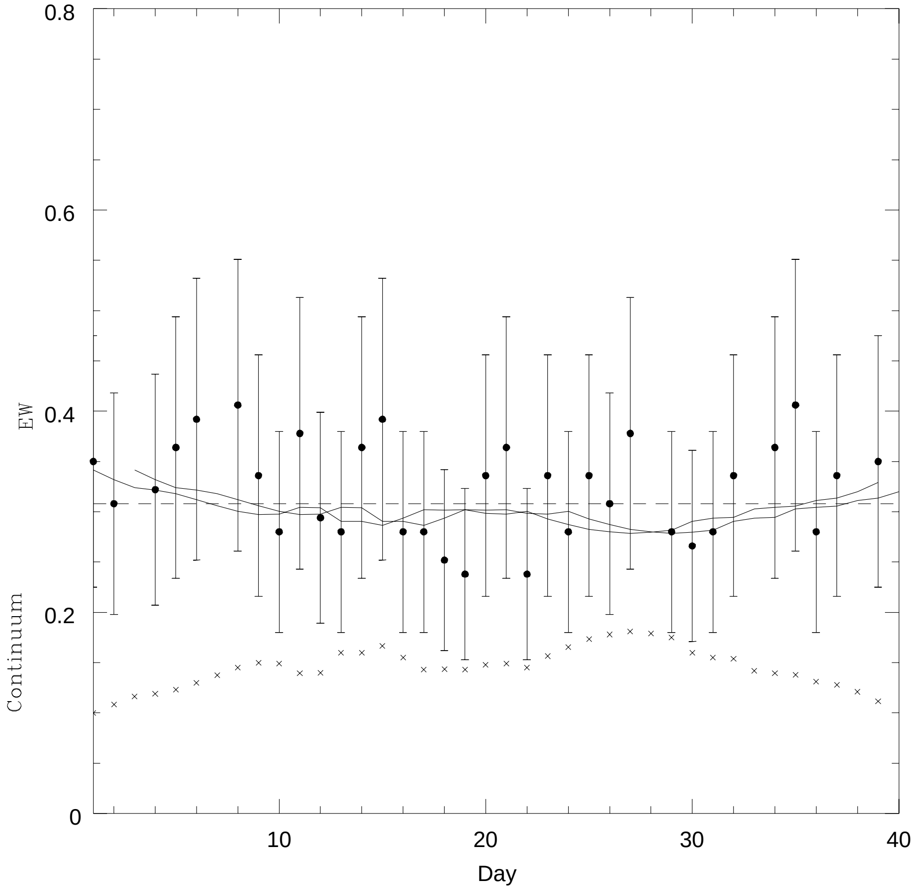
0.8
0.6
0.4
0.2
0
EW
Continuum
10
20
30
40
Day